A SLITLESS, INTENSIFIED READOUT, GATED SPECTROMETER: WAVELENGTH AND EFFICIENCY CALIBRATION, TIME RESPONSE CHARACTERIZATION

Michel Gerassimenko and Mark C. Fowler

June 1986

DISCLAIMER

To: All holders of UCRL-94098 Preprint, "A slitless, intensified readout, gated spectrometer: wavelength and efficiency calibration, time response ch racterization."

From: Technical Information Department

ERRATA

Page 2

Paragraph 5: the formula InSnO was incorrectly given for indium tin oxide.

Paragraph 7: λ = 265 nm, not 256 nm.

Figure 2 caption should read as follows: Universal efficiency curve (adapted from published data[3]) for a perfectly conducting blazed grating with a 90 deg apex used in the scalar domain (i. e., $\lambda/d < 0.2$). The equation marking the x-axis consists of two terms: the first follows directly from the fundamental grating equation (where m is the order, λ the wavelength, d the spacing between grooves, and θ_B the blaze angle), and the second accounts for configurations other than Littrow. Finite conductivity makes the peak efficiency equal to the material reflectivity.

Page 5

Figures 8 and 9 have been reversed.

These changes have been incorporated into the forthcoming article, which was prepared for the Society for Photo-optical Instrumentation Engineers (SPIE) 30th Annual Symposium.

Technical Information Department

A slitless, intensified readout, gated spectrometer: wavelength and efficiency calibration, time response characterization

Michel Gerassimenko and Mark C. Fowler

University of California, Lawrence Livermore National Laboratory
Mail Stop 43, P.O. Box 808, Livermore, California 94550

Abstract

A spectrometer has been developed specifically for the x-ray laser effort at Lawrence Livermore National Laboratory (LLNL). The instrument takes advantage of the small divergence and size of the lasing source by positioning all three components—the source, a custom-ruled grating, and a microchannel plate (MCP) detector—on the Rowland circle. The sum of incident and diffracted angles is kept constant. Illuminating a pinhole at the source location with a z-pinch produces wavelength calibration at several energy ranges in the 65- to 200-eV interval. The same source used in conjunction with the MCP camera and Kodak 101 film yields the absolute detector efficiency. Ion bombardment of a beryllium target at the source location produces the x-rays necessary to determine the absolute efficiency of the grating-detector combination at 107 eV. Grating efficiency is then deduced from the MCP efficiency at that energy. Three 25-Ω stripline structures on the MCP allow sub-nanosecond gating of the spectrometer, which improves the signal-to-background ratio. The rise time response of the entire MCP detector-cable assembly is about 200 ps. We also measured the transmission of the filters that are used in suppressing ultraviolet backgrounds.

Introduction

Soft x-ray lasing has been demonstrated using laser-illuminated targets, where the length of the illuminated medium is typically 1 cm, and the predicted divergence of the output beam is about 10 mrad.[1,2] The lasing lines for such a scheme are narrow (typically Doppler broadened to $\Delta\lambda/\lambda \simeq 10^{-4}$), and last for tens of picoseconds. The target material, on the other hand, takes nanoseconds to cool below 20–50 eV, and so emits background radiation in the energy range of interest much longer than the soft x-ray laser.

The narrow source line is superimposed on the broad background emission of the target. Under these conditions the instrument's sensitivity is directly proportional to its spectral resolution (at least for resolving power less than 10^4). The sensitivity is also influenced by the spectrometer's time resolution or discrimination. High sensitivity is desirable for detecting line and continuum emission from the target; it is absolutely essential to detect even weakly amplified lines.

The instrument

Given the above considerations, the x-ray laser effort at LLNL called for an instrument of high sensitivity and high resolution (spectral and temporal). In pursuing a number of proposed lasing schemes, we were called on to observe output radiation at several narrow energy ranges within the 65- to 200-eV interval. Since these requirements could not be met by any commercially available instrument, it was necessary to develop a spectrometer of our own.

Figure 1 is a schematic of the Slitless Intensified Readout GAted Spectrometer (SIRGAS), an instrument that was built to meet these requirements. The basic design takes advantage of the small source size (roughly 100 μ) by positioning all three components—the lasing source, the grating, and the detector—on the Rowland circle. This configuration eliminates the need for a slit.
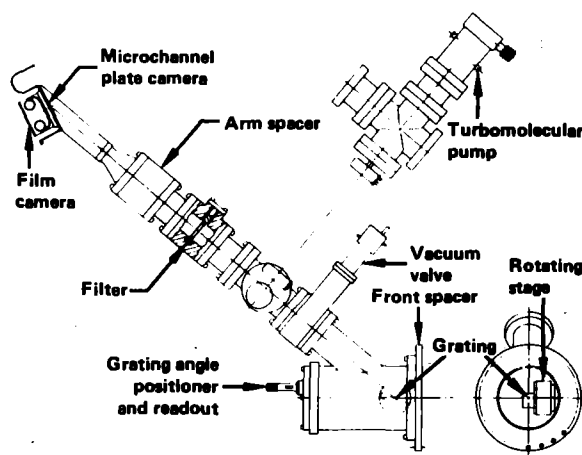

Figure 1. The SIRGAS spectrometer. The basic design, by placing the source, grating, and MCP detector on the Roland circle, eliminates the need for a slit.

The grating is made just large enough to intercept the entire laser footprint, and the detector consists of a proximity-focused, gated MCP camera. Since the desired coverage extends to nearly 200 eV, grating efficiencies are quite good for grazing angles up to about 20 deg. For energies of interest, the angle of incidence (α) and the angle of refraction (β) are within a few degrees of each other. We chose to operate in the $\beta < \alpha$ mode with $\alpha + \beta = 139.3$ deg. Geometric considerations force the grating outside the target chamber radius (roughly 80 cm), so that $R \simeq 3$ m for the chosen value of α.

Although the target chamber is now part of the spectrometer, the grating is mounted on a rotating stage so that α can be changed with a compensating change in β. Thus, by rotating the grating and changing two spacers (one between the target chamber port and SIRGAS, the other in SIRGAS's arm), all of the relevant pieces of the instrument are kept on the Rowland circle. Different energy ranges are accessed by selecting α and the appropriate grating. Grating efficiency is maximized by operating close to the peak shown in Figure 2 (after Loewen and Neviere[3]). Finite conductivity makes this peak efficiency equal to the material reflectivity.

Due to grating unavailability we had custom masters ruled at Hyperfine Inc and used replicas of these masters in SIRGAS. The ruled area is 2-cm wide and extends over 3.5 cm. Five energy ranges which were deemed of interest prior to the experimental series are covered using the three different gratings shown in Table 1.

Photons diffracted by the grating are detected by the MCP camera[4] (sketched in Figure 3). The back of the MCP is coated with gold roughly 1-μ thick, and so are the three 3.1-mm-wide, 25-Ω strips. The distance between the strips is 2.4 mm. So as not to degrade the time response of the camera, great care is taken to properly match the various electrical components. Each strip, combined with the conductive backplane, constitutes a 25-Ω structure, and each is in contact with a 25-Ω structure on the printed circuit board. The resulting striplines are each in turn connected to 25-Ω semi-rigid cables at each end. Matched SMA connectors are used throughout.

Separated by 0.5 mm from the MCP is a fiber optic faceplate, which constitutes an interface between the camera vacuum and the film magazine (which is in air). The faceplate is coated with InSnO for conductivity. A P11 phosphor is deposited on the faceplate to convert the electrons that are produced by the MCP into light. This light is then recorded on 2484 film pressed against the back of the faceplate.

A 10-mrad-divergence source produces lines which are roughly 20-mm long at the MCP, and which thus intercept all three strips. Gating is accomplished by supplying suitable pulses to each stripline. For the experimental series on the Novette laser at LLNL we applied voltage to the MCP for nearly 1 μs before the laser shot took place, using an Auston switch to short the voltage across the MCP to ground. The relative gating of each strip was controlled by the length of semi-rigid cable between it and the Auston switch. Typically a 500 ps delay between strips was used (i.e., strip 1 was switched on from 0 to t_0, strip 2 from 0 to t_0 + 500 ps, etc.).

The target was illuminated with 530-nm green light. Although the MCP camera is insensitive to this wavelength of light, it is exceedingly sensitive to the ubiquitous second harmonic at $\lambda = 256$ nm. The problem, therefore, was to cut down on the 256-nm light while transmitting as much radiation as possible in the x-ray energy range of interest (i.e., 65- to 200-eV). The manufacturer specifications and calculated transmissions of the filters that were used to solve this problem are listed in Table 2.
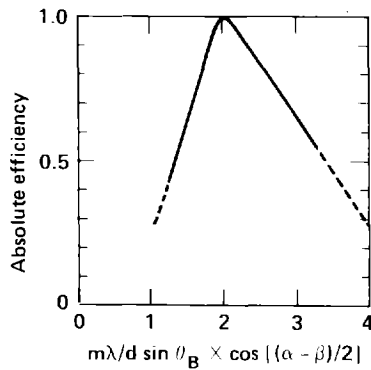

Figure 2. Universal efficiency curve for a perfectly conducting blazed grating (adapted from published data[3]). The equation marking the x-axis consists of two terms: the first follows directly from the fundamental grating equation ($m\lambda = d\sin\theta$, where m is the order of the wave, λ = source wavelength, and d = spacing between grooves), and the second accounts for configurations other than Littrow. The blaze angle is given by θ_B. The curve shows a 90-deg apex when the grating is used in the scalar domain (i.e., $\lambda/d < 0.2$).

x-axis label: $m\lambda/d \sin \theta_B \times \cos |(\alpha - \beta)/2|$

Table 1. Spectrometer Parameters in 5 Energy Ranges.

Energy (eV)	α_c (deg)	β_c (deg)	Grating 1/mm	Grating blaze (deg)	Distance a (cm)	Distance b (cm)
65–74	73.1	66.2	2400	3	87.1	121.0
88–104	72.2	67.1	2400	3	91.5	116.8
113–130	72.7	66.6	3600	3	89.2	119.1
140–167	72.1	67.2	3600	2,3	92.3	116.1
170–210	71.6	67.6	3600	2	94.7	113.8

α_c = Angle of incidence, with respect to the normal, at grating encter.
β_c = Angle of refraction, with respect to the normal, at grating center.
a = Source to grating center distance.
b = Grating center to detector center distance.

Calibrations

Extensive calibrations have been carried out in the energy ranges listed in Table 1. In what follows, we discuss the technique used in each type of calibration and present sample data and results.

Many of of the calibrations are performed on a laboratory setup where a pinhole is placed at the source location (i.e., the same position, relative to the grating, as the x-ray laser target. A z-pinch, which produces a rich spectrum of O, N and Aℓ lines superimposed on a continuum in the 80- to 3000-Å range, back-illuminates the pinhole. The arrangement is sketched in Figure 4. The pinhole is a crucial element of the setup. It mimics the small source size essential to the working of the spectrometer and represents a very low conductance path between the high vacuum environment of the grating and MCP camera and the low vacuum pinch source. The pinch source operation relies on breakdown of the residual gases (primarily oxygen and nitrogen) within an alumina tube. The presence of these gases, along with the tube composition, explains the the observed spectrum of O, N, and Aℓ lines. For breakdown to occur, the source must be operated at the mTorr pressure level.
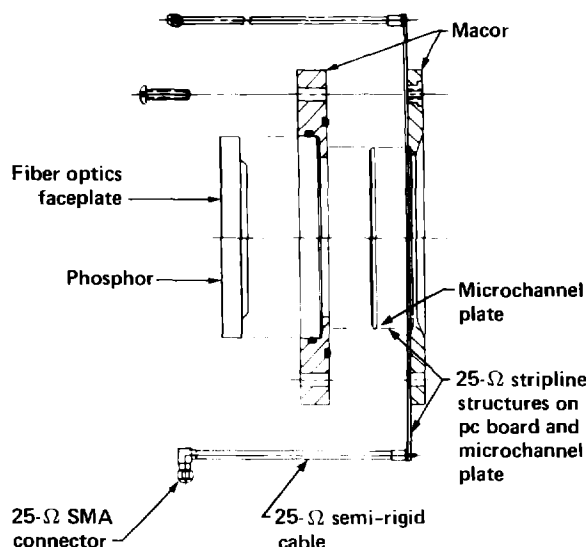

Figure 3. The microchannel plate camera (MCP). There are three independently gateable 25-Ω structures. A fast film (Kodak 2484) is pressed against the back of the fiber optic faceplate to record light produced by the P11 phosphor.
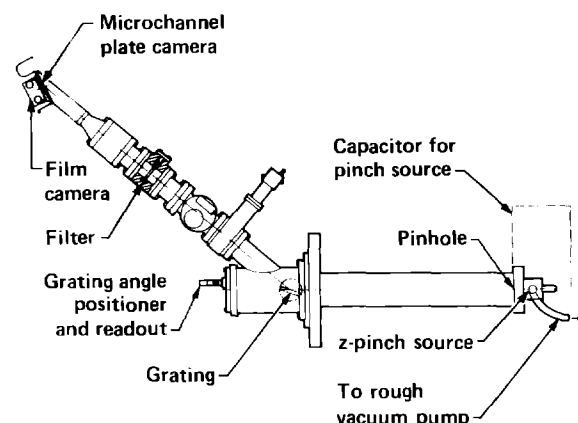

Figure 4. The calibration setup. A z-pinch source back-illuminates the pinhole.

Table 2. Filter Characteristics.

Filter	Calculated Transmission at Indicated Energy			
	4.7 eV	70 eV	120 eV	150 eV
3000 Å CH/600 Å Al	3×10^{-5}	0.2	0.1	0.2
3000 Å CH/500 Å Mo	2×10^{-5}	0.04	0.4	0.5
5000 Å Be	—	0.2	10^{-6}	10^{-4}

Wavelength and energy resolution

Wavelength calibration is accomplished by simply recording the pinch spectrum and the zero order image at known grating angular positions. Sample spectra at 104 Å and 172 Å recorded on Kodak 101 film are shown in Figure 5. The positioning accuracy of the grating is limited to 0.01 deg by the readout resolution of the rotating stage. This limiting value corresponds to (roughly) 0.3 Å for the 3600 ℓ/mm gratings and 0.5 Å for those ruled at 2400 ℓ/mm. Tests show that line positions are repeatable to this level by simply dialing the desired angle. This is the minimum wavelength accuracy that can be achieved when no additional information is available (i.e., when only a single line has been obtained after moving the grating angle). In practice many lines from the target materials are recorded. Their known wavelengths can greatly improve the spectrometer's wavelength calibration.

The expected source size of 100 μ is the limiting factor in SIRGAS's energy resolution. The data shown in Figure 5 were obtained with a 50-μ pinhole at the source position. For this size source the resolving power is clearly several thousand.

MCP camera efficiency

A similar setup (z-pinch illuminating a pinhole) is used to determine the MCP camera efficiency. The calibration is in two steps. First, simply alternating the MCP camera and the Kodak 101 film at the detector plane yields their relative efficiency. Since the film's sensitivity has been determined under appropriate development conditions,[5] the MCP camera absolute efficiency is easily derived.

With about 1.1 kV across the MCP and 3 kV between the back of the MCP and the phosphor, the camera can be operated with enough gain for single photons to produce discernible dots on the 2484 film. A portion of a spectrum containing VI lines is shown in Figure 6. Figure 7 is a 101 film record of these same lines.

Figure 8 is a microdensitometer scan across the lines shown in Figure 7. Given the reported film sensitivity[5] and the mathematical model of its x-ray response,[6] the detector plane flux can be derived from the specular film density. The observed excess density of 0.23 at the 66.3-deg angle of incidence to the normal yields a detector plane flux of 6×10^{-3} photons/μ^2/discharge.

Counting the single photon records on 2484 film (reproduced in Figure 6), we get 10 dots for each millimeter along the 115.8-Å line. Combining this result with the measured 180-μ full width at half maximum of the line (Figure 8) we obtain an MCP efficiency of 1% at 107 eV (i.e., 115.8 Å). Such an efficiency is quite reasonable given: (a) the 4% reported quantum efficiency for Au at 107 eV (Reference 7) and, (b) the 40% fractional area of channels within the MCP.

Grating efficiency

A beryllium target is placed at the source location and bombarded with ions to produce a 1/8-inch-diameter source of Be K x-rays. The x-ray flux at the grating of SIRGAS is determined by placing a calibrated proportional counter at a symmetrical position with respect to the source. The large source size results in a very broad line at the image plane, as shown in Figure 9. Single photon events are readily discernible on the MCP camera film record, an enlargement of which is displayed in Figure 10. The x-ray flux at the grating and the single photon event density yield the product of the grating and MCP camera efficiencies: roughly 10^{-3} at 107 eV. Given the MCP camera efficiency determined above we deduce a grating efficiency of close to 10%.
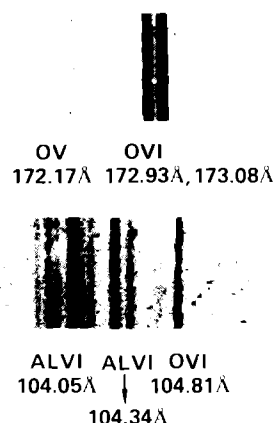

OV   OVI
172.17Å 172.93Å,173.08Å

ALVI ALVI OVI
104.05Å | 104.81Å
104.34Å

Figure 5. Kodak 101 film data obtained by back-illuminating a 50-μ pinhole at the source location with a z-pinch. Simply recording the pinch spectrum and the zero order image at known grating positions yields wavelength calibration. Sample spectra from ionized oxygen and aluminum are shown.
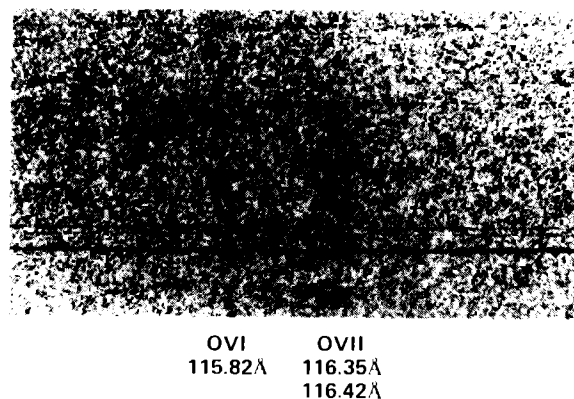

OVI   OVII
115.82Å 116.35Å
116.42Å

Figure 6. MCP camera data obtained by back-illuminating a 50-μ pinhole at the source location with a z-pinch. The black dots are single photon events.
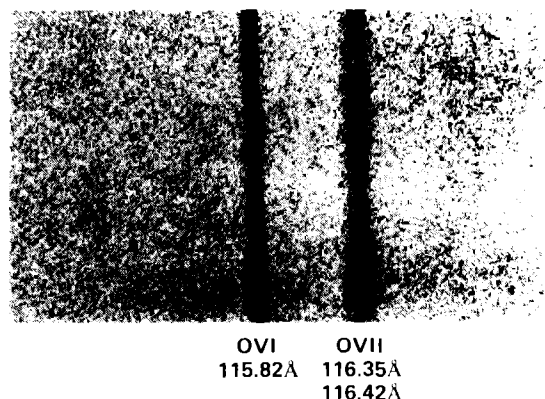

OVI   OVII
115.82Å 116.35Å
116.42Å

Figure 7. 101 film record of the lines shown in Figure 6.

The photon grazing angle of incidence upon the grating is 17 deg and the grating blaze is 3 deg, so the effective angle of incidence on a grating groove is 20 deg. The grating is operated sufficiently close to its blaze wavelength, so that (according to Figure 2) its calculated efficiency should be the reflectivity of gold (i.e., about 30% at 107 eV). Although the efficiency shown in Figure 2 is strictly applicable for conditions nearer normal incidence, it is gratifying to measure an efficiency at a 70 deg angle of incidence which is a reasonable fraction of the maximum efficiency attainable.

MCP camera time response

The time response of the MCP camera, considered together with the striplines and associated cables, is determined using a time domain reflectometer to propagate very fast pulses through the camera. Examination of the pulse after passage through the camera provides a measure of the time response of the entire system. A typical response is shown in Figure 11. The 10 to 90% rise time is about 150 ps. During actual use on the Novette laser, a voltage is applied prior to the shot and an Auston switch sequentially grounds the striplines (see the above discussion, under the heading "The instrument"). Since the MCP gain is a highly non-linear function of voltage, the actual turn-off time of the MCP is substantially shortened. Each of the striplines on the MCP camera can be gated off within a period of 100 ps. This is about the difference in light transit time between photons arriving at the low and high wavelength positions on the detector plane.

Filter transmission

Filter transmission is determined using the z-pinch source to back-illuminate a pinhole or a slit. Visual matching of the records obtained with the same detector but summed over different numbers of discharges with and without the filter, yields the transmission. Examples of such data are shown in Figure 12.

The specular density in excess of background is nearly identical for the 1-discharge record with no filter and the 16-discharge record with the filter. The transmission of the 600-Å Aℓ on a 3000-Å CH filter is determined to be about 0.06 at 75 eV. Even though the filter is primarily designed for use below the Aℓ edge at 73 eV, the transmission measured at 75 eV agrees with the value of 0.06 calculated using nominal values for the material thicknesses.
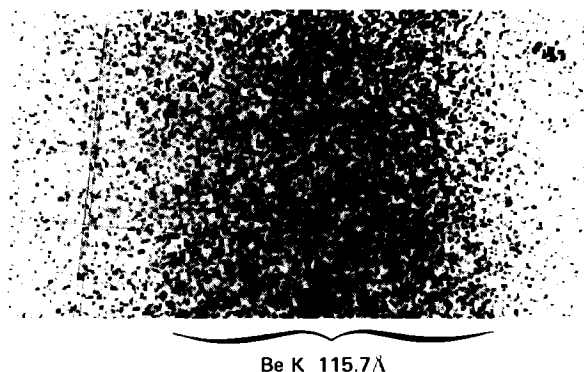

Be K 115.7Å

Figure 8.   Microdensitometer data showing the specular density for a scan across the 101 film data shown in Figure 7.
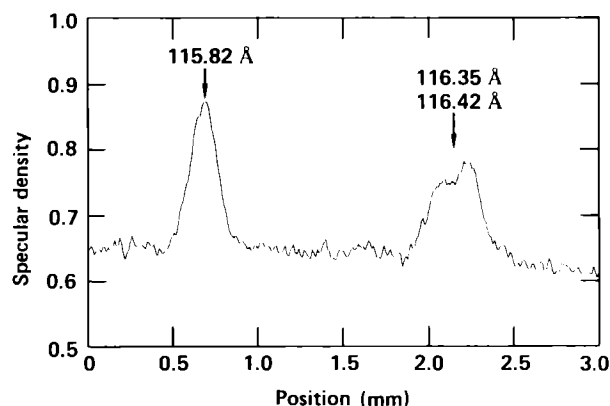

Figure 9.   Detector plane image of large (1/8-inch-diameter) Be K x-ray source.
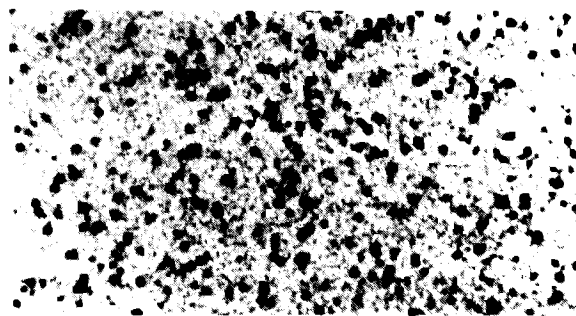

Figure 10.   Enlargement of a portion of data similar to that of Figure 9, but of shorter exposure to show single photon records.
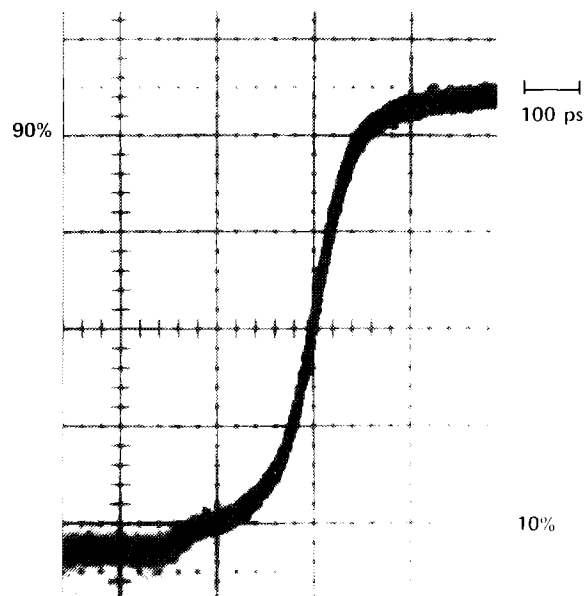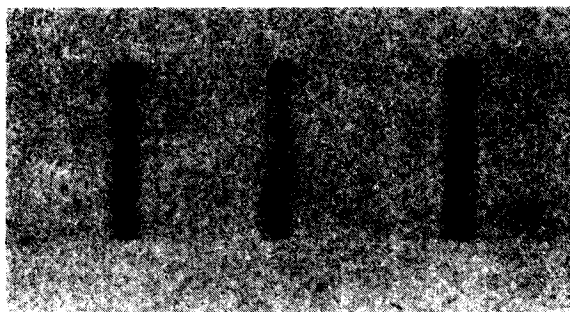
Figure 11.   Time response of a typical stripline-cable assembly. The 10-90% rise time is roughly 150 ps. during actual use on the Novette laser, voltage was applied prior to the shot and an Auston switch was used to sequentially ground the striplines.
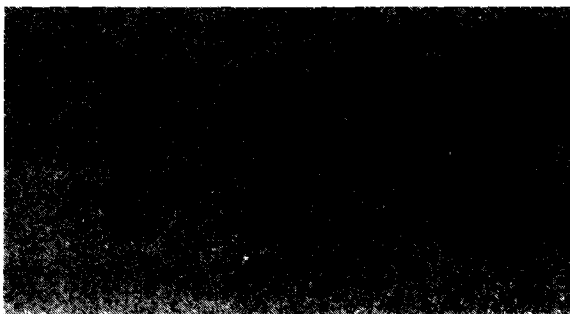
16 discharges with filter

| OV | OV | OV |
| 164.6Å | 166.2Å | 168.0Å |

1 discharge without filter

Figure 12.   MCP camera data with and without a 600-Å Aℓ on 3000-Å CH-filter. All blends of several closely spaced OV lines are recorded.

Conclusions

We have developed a novel spectrometer specifically for the x-ray laser effort at LLNL. Calibrations in the 65- to 200-eV range have been carried out which, in the absence of reference lines, produce an absolute wavelength accuracy of 0.3 Å and demonstrate a resolving power of several thousand. The MCP camera can detect single photons with an efficiency of about 1% at 107 eV. It is gateable at the 100-ps level. The grating efficiency is approximately 10% at 107 eV. Transmission of the filters that are used to suppress UV backgrounds is nominal.

Acknowledgments

References

1. Rosen, M. D., et.al., "Demonstration of a Soft X-ray Amplifier," Phys. Rev. Lett., Vol. 54, p. 106. 1985.

2. Matthews, D. L., et.al., "Exploding-Foil Technique for Achieving a Soft X-ray Laser," Phys. Rev. Lett., Vol. 54, p. 110. 1985.

3. Loewen, E. G., and M. Neviere, "Simple Selection Rules for VUV and XUV Diffraction Gratings," Appl. Optics, Vol. 17, p. 1077. 1978.

4. Stewart, R. E., R. Booth, D. D. Dietrich, R. J. Fortner, R. E. Marrs, and D. F. Price, "Multi-frame Nanosecond Camera Using a Single Microchannel Plate," Lawrence Livermore National Laboratory, Livermore, CA, UCRL-88580. 1983.

5. Henke, B. L., F. G. Fujiwara, M. A. Tester, C. H. Dittmore, and M. A. Palmer, "Low-energy X-ray Response of Photographic Films, II. Experimental Characterization," J. Opt. Soc. Am., B1, p. 828. 1984.

6. Henke, B. L., S. L. Kwok, J. Y. Uejio, M. T. Yamada, and G. C. Young, "Low-energy X-ray Response of Photographic Films, I. Mathematical Models," J. Opt. Soc. Am., B1, p. 818. 1984.

7. R. H. Day, "Photoemission Measurements for Low Energy X-ray Detector Applications," AIP Conf. Proc., No. 75, p. 44. 1981.